Fuel 117 (2014) 1115–1129

Contents lists available at ScienceDirect

Fuel

journal homepage: www.elsevier.com/locate/fuel

Total porosity measurement in gas shales by the water immersion porosimetry (WIP) method

Utpalendu Kuila [a,*], Douglas K. McCarty [b], Arkadiusz Derkowski [c], Timothy B. Fischer [b], Manika Prasad [a]

[a] Department of Petroleum Engineering, Colorado School of Mines, Golden, CO 80401, USA
[b] Chevron ETC, 3901 Briarpark, Houston, Texas 77042, USA
[c] Institute of Geological Sciences, Polish Academy of Sciences, Research Centre in Kraków, Senacka 1, PL-31002 Kraków, Poland

HIGHLIGHTS

- Total porosity measurement for gas shales without using crushed rock is presented.
- The method uses a modified saturation – immersion technique with deionized water.
- Porosity values are reproducible within a low average absolute uncertainty.
- Swelling in gas shales during saturation with deionized water is not significant.
- Solvent extraction pretreatment can remove solid organic matter.

ARTICLE INFO

Article history:
Received 22 April 2013
Received in revised form 10 September 2013
Accepted 20 September 2013
Available online 15 October 2013

Keywords:
Gas shales
Porosity
GRI
Water immersion porosimetry (WIP)
Haynesville

ABSTRACT

Over the past decade interest in shale properties has increased due to the commercial success of gas shale plays. Despite their commercial importance, porosity measurement from gas shale samples is still challenging due to their extremely low permeability and complex pore structure. This leads to a significant uncertainty in the economic assessment of these plays. The current energy industry standard technique for measuring porosity in gas shales is based on methodology developed by the Gas Research Institute (GRI) that involves crushing a rock and aggressive pretreatment. The objective of this study is to develop an alternative method of measuring total porosity in gas shales. A porosity measurement using a liquid saturation and immersion technique with deionized water was adopted and modified for such applications. The water immersion porosimetry (WIP) technique was used to measure total porosity of shale samples from an Eastern Europe Silurian gas shale play and the Haynesville Shale from East Texas, USA. The samples were characterized for whole rock quantitative mineral and elemental composition, along with cation exchange capacity (CEC) and organic matter. The results from the WIP measurements are compared with other standard techniques including the GRI method and mercury intrusion porosimetry (MIP). An assessment of the advantages, potential errors, pitfalls and reproducibility of this method are also presented.

The experimental results indicate that WIP provides (i) highly reproducible porosity, grain density, and bulk density measurements for gas shales, (ii) the average absolute experimental uncertainty is ±0.22 porosity unit (p.u.), compared to the reported uncertainty level of 0.5 p.u. for GRI measurements, (iii) standard MIP techniques systematically underestimate the porosity and grain density compared to WIP, because mercury cannot access the entire pore structure in shales, and (iv) grain density values obtained by the GRI method in samples with high organic matter content are higher compared to WIP measurements, probably because of dissolution of solid organic matter during solvent extraction pretreatment.

1. Introduction

Porosity is the most fundamental hydrocarbon reservoir property, which has both scientific and economic implications. Porosity control or influence physical properties including geo-mechanical behavior and fluid transport. Accurate porosity measurements are also important for resource evaluation and reserve calculations. The commercial success of gas shale and liquid rich shale plays has stimulated interest in gaining more understanding of their physical properties. Shale reservoirs are typically rich in organic matter, often with more than 2 wt.% total organic carbon (TOC), and have

* Corresponding author. Tel.: +1 3036699651.
E-mail address: ukuila@mymail.mines.edu (U. Kuila).

0016-2361/$ - see front matter © 2013 Elsevier Ltd. All rights reserved.
http://dx.doi.org/10.1016/j.fuel.2013.09.073

lower porosity (1–10 porosity units[1]) compared to conventional reservoirs. Porosity measurement uncertainty that is acceptable for high porosity conventional reservoirs (>15 p.u.) is inadequate for evaluating shale reservoirs because of the low total porosity.

1.1. Porosity in organic-rich shales

Porosity is defined as the percentage of the pore or void volume of the porous sample over the bulk volume. A pore is the part of rock occupied by fluids. This definition is complicated in shales because of the presence of clay minerals and the variability of organic matter (OM). Exchangeable cations associated with expandable clay minerals have strongly bound shells of water molecules where the quantity varies depending on the water activity of the system. Thus, total porosity is the water content having molecular interaction with clay minerals, plus the free fluid (water, gaseous and liquid hydrocarbons) in the relatively larger open pore and capillary spaces.

Organic matter (OM) in these shale formations is a mixture of different organic compounds that have different rheological properties. Bitumen is often classified as being soluble in organic solvents, whereas kerogen is the insoluble organic component. However, this classification does not indicate whether they are solid or fluid. Bitumen can have both solid [2] or plastic characteristics depending on the pressure and temperature conditions. In this study, fluid and solid organic compounds are operationally defined based on the S1 and S2 components in RockEval pyrograms, respectively. Thus, compounds that produce a peak in the S2 region of RockEval, which is thermally stable above 300 °C, should be considered as a part of the solid matrix of the rock.

1.2. Challenges with previous porosity measurement techniques for shales

Direct porosity measurement in shales is complicated because of the fine grained texture, extremely low permeability, high OM content and the strong interaction with water molecules. The current energy industry standard porosity measurement protocol for gas shales is based on a helium pycnometry technique developed by the Gas Research Institute (GRI) [3–5]. The GRI method measures bulk density by mercury immersion using Archimedes' Principle on a large (~300 g) block of intact untreated core material. The sample is then crushed, followed by solvent extraction with hot toluene by the Dean Stark method, and then dried in an oven at 110 °C to remove pore fluids. Grain volume of the pretreated crushed material is measured by helium pycnometry and Boyle's law. Because of the nanodarcy permeability of these formations, crushing is used to accelerate the extraction of the formation fluids and to facilitate helium intrusion in the pore space during the grain volume measurement [3]. Pore volume is calculated using the difference between bulk volume and grain volume.

Significant discrepancies exist in porosity and grain density values of comparable samples measured by different commercial laboratories using the GRI method [6–9]. There are significant potential sources of errors in the GRI procedure (see GRI workflow chart in Appendix A):

1. The crushing procedure is not standardized. Inconsistent crushing and sample handling procedures can introduce a sampling bias including altering the native saturation.
2. Clay bearing rocks have high micro- and meso-porosity[2] and cation exchange capacity (CEC) making them sensitive to variable hydration states depending on the relative humidity (RH) of the measurement environment. Exposure to ambient humidity during crushing and sample handling prior to helium pycnometric measurement may alter the native saturation and can significantly affect the measured grain density and produce high uncertainty in porosity calculations.
3. The solvent extraction pretreatment may potentially remove some of the solid organic matter which may artificially increase the porosity.

Mercury intrusion porosimetry (MIP) is a widely accepted method to measure porosity and pore size distribution for conventional reservoir rocks like sandstones and limestones. MIP in shales, however, significantly underestimates porosity [10–13] because of incomplete mercury intrusion into fine pore system, compression of the rock framework, and the potential for opening closed pores under the high pressures used (up to 414 MPa). In crushed shales, the pore volume measured using MIP increases with a decreasing mean particle size of the crushed samples [12]. The increase in the measured pore volume is related to better pore accessibility in the smaller crushed particle size, but there also may be additional creation of pore space during the crushing process [12].

1.3. Objective of this study

The purpose of this study was to develop an alternative total porosity measurement method for gas shales. A liquid saturation and immersion technique was optimized and deionized water was used for both the saturating and the immersing fluid. A systematic study of the technique, including evaluating the reproducibility and experimental uncertainty, was conducted on two sets of shale samples, an Eastern European Silurian gas shale formation and the Haynesville Formation of East Texas, USA. The results were compared and discussed with those measured using the GRI and MIP techniques on samples from the same core depth.

2. Porosity measurement by the liquid saturation and immersion technique

The saturation and immersion technique determines porosity by saturating a sample with a liquid of known density, and calculating the pore volume from the weight difference between the fully saturated and dry states. The total volume of the sample is determined by immersing it in the fluid using Archimedes' Principle. Thus, bulk density, grain density, and porosity are determined from the same experimental sample. This technique has been recommended as a standard porosity measurement by the American Petroleum Institute (API) [14], the American Society for Testing and Materials [15,16], and the International Society for Rock Mechanics [17]. The method has been employed in analysis of a wide variety of rock types including low porosity granites [18–20], cations attached to the highoil sands and sandstones [21,22], dolomites and limestones [23], and shales [24–32]. The two most important experimental details that needs to be considered are the choice of saturating and immersing fluid, and the pretreatment conditions.

2.1. Choice of saturating and immersing fluids

Previous studies used different saturating and immersing fluids that include acetylene tetrachloride [21]; deionized (DI) water [18–20,23,24,28–31,33], light hydrocarbon [25,27], kerosene [26,32] and other petroleum products and paraffin [34,35]. The API Recommended Practices 40 document [14] suggests using brine, light refined oil, or a high-boiling point solvent as a saturating and immersion fluid. An ideal saturating fluid should have the following properties:

[1] Porosity unit: "A unit equal to the percentage of pore space in a unit volume of rock. It is abbreviated to p.u. and lies between 0 and 100" [1]

[2] Pore-size classification following the International Union of Pure and Applied Chemistry (IUPAC): (i) Micropore: pore-size <2 nm; (ii) mesopore: pore-size 2–50 nm; (iii) macropore: pore-size >50 nm.

- low surface tension and a high wetting tendency,
- low viscosity,
- a high vapor pressure and slow evaporation rate,
- low reactivity with the porous material,
- stable composition and density,
- be non-hazardous and have safe handling properties.

The driving forces to saturate porous media are the pressure gradient and the surface tension of the liquid. The coefficient of penetration [34] for a wetting liquid into a capillary system, assuming a zero contact angle, is defined by the following relation:

$$z = \frac{\gamma}{2\eta} \quad (1)$$

where γ is the surface tension of the fluid in dyne/cm, η is the dynamic viscosity of the fluid in poise (dyne s/cm^2), and z is the coefficient of penetration in cm/s. Higher penetration coefficients of DI water compared to other commonly used fluids means there is faster penetration into the micropores and capillaries (Table 1).

The polar nature of water molecules has a strong affinity for exchangeable cations attached to the high surface area of clay minerals. Thus, saturating the pore system with water is ideal because it will penetrate small pores and capillaries associated with clay mineral aggregates. Using DI water as opposed to brines [14] for shales is justified because the goal is to measure total porosity including free and clay bound water (CBW). Saturation with any brine solution can also cause complicating cation exchange reactions. Using a potassium-rich brine would change the natural cation composition and affect the CBW content due to significantly lower K hydration enthalpy compared to Ca and Na (for example, Sato et al. [36]). The properties of DI water (i.e. density) are stable and it is easier to obtain a standardized DI water than a consistent KCl brine solution. Because water is used as both the saturating and immersing fluid, this procedure can thus be referred to as the water immersion porosimetry (WIP) technique. A possible drawback of using water as the saturating fluid is the potential swelling of the bulk rock due to clay mineral expandability, osmotic swelling or simple mechanical expansion during the saturation process. Experiments were designed to test bulk rock swelling and its possible effect on the porosity measurements and will be discussed later.

2.2. Pretreatment conditions

All porosity measurement techniques involve removal of naturally occurring formation fluids, before saturating the pore system with a measurable quantity of external fluid. Solvent extraction using a Soxhlet or Dean Stark apparatus, or distillation by heating or a combination of both are used to remove formation fluids, including water and hydrocarbons. The abundance of chemically heterogeneous OM in organic rich gas shale formations must be considered in the choice of the pretreatment techniques. Solvent extraction and distillation by heating remove different components of the residual oil and organic matter [37–39]. Heating at 200 °C removes volatile hydrocarbons in the C5–C25 composition range [40], whereas solvent extraction removes the volatile hydrocarbons and the "heavy-end" C10–C40+ components, including non-volatile asphaltenes and high molecular weight polar nitrogen, sulfur, and oxygen (NSO) compounds [41]. Comparisons between RockEval pyrograms of natural and toluene treated (using the Dean Stark technique) aliquouts from the same shale sample indicate that there is a significant loss of the S2 component (Fig. 1). The difference in the S2 pyrogram patterns at temperatures <400 °C after Dean Stark indicates that a part of solid organic matter is dissolved in the solvent extraction process. Therefore, pretreatment using distillation by heating method was opted over the solvent extraction techniques.

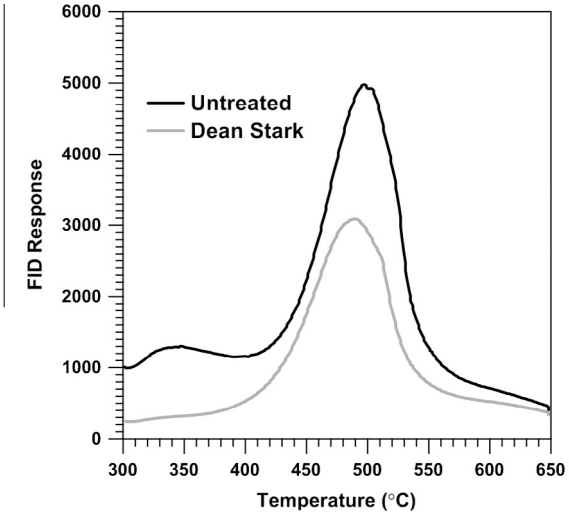

	S1	S2	S3	TMAX	LECO TOC	HI	OI
Natural	3.01	3.55	0.40	457	2.73	130	15
Dean Stark	0.76	1.98	0.31	449	2.61	76	12

Fig. 1. Comparison of RockEval II tabulated data and S2 pyrograms between a representative natural shale and an aliquot sample after Dean Stark extraction.

The heating temperature for pretreatment must be high enough to remove volatile hydrocarbons and adsorbed water hydrating clay minerals, but not so high as to alter the solid organic and inorganic framework. Luffel et al. [5], and Luffel and Guidry [4] suggested a pretreatment temperature of 110 °C in their GRI methodology, which is similar to the API recommendation [14], but not all clay-bound water can be removed by heating at 110 °C. Smectite and mixed-layered illite–smectite clay structures are capable of retaining significant amount of electrostatic bound water as strongly held exchange cation hydration spheres in excess of 200 °C [42–44]. Heating at 200 °C is selected, based on the

Table 1
Penetration coefficient [34] of commonly used saturating fluid for liquid-saturation and immersion techniques, assuming the contact angle to be zero.

Liquid	Surface tension (dyne s/cm)	Dynamic viscosity (centipoise)	Penetration coeffiecient (cm/s)	Vapor pressure (mmHg)
Acetelyene tetrachloride	31.1	1.610	965.6	72.37
DI water	72.7	1.002	3630.9	17.55
Kerosene	27.5	1.233	1115.2	2.21
Light hydrocarbon				
n-Hexane	18.5	0.312	2964.7	121.41
Octane	21.6	0.541	1998.1	10.43
Decane	23.8	0.912	1305.5	0.96
Isopar V	27.0	18.005	75.0	<0.08

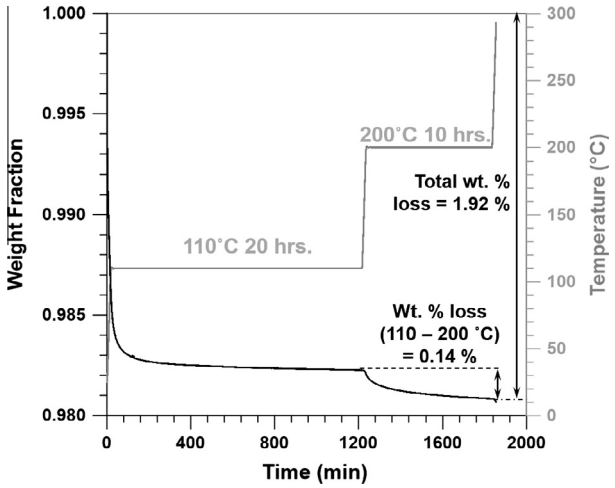

Fig. 2. TGA curve (black) for a representative shale sample from the Haynesville Formation using a heating protocol as shown by the temperature curve (grey). Total weight loss from start to 200 °C and weight loss from 110 to 200 °C are shown.

recommendation of Środoń and McCarty [43], as it removes the majority of clay bound water without altering the clay mineral structure by dehyrdoxylation. Luffel and Guidry [3], in their original GRI report, also suggested preheating at 204 °C. Thermogravimetrimetric (TGA) measurements on an illitic shale from the Haynesville Formation suggest significant dehydration mass loss of about 0.14% happens between 110 °C and 200 °C (Fig. 2). Consistent RockEval II S2 and S3 values between untreated and 200 °C preheated aliquots of several organic rich shale samples with variable OM maturation level proves that preheating at 200 °C does not alter the solid OM in the rock (Fig. 3).

3. Methods and materials

3.1. Sample characterization

A sub-sample from each core depth was ground to <425 μm (<40 mesh) powder, homogenized, and divided to obtain mineralogically and chemically representative homogeneous splits [45], which are then used for the various analyses. Quantitative mineral concentrations were obtained by X-ray diffraction (QXRD) analysis of randomly oriented powders spiked with 10% by weight ZnO, and the proprietary Chevron computer program Quanta [46,47]. In this method, all dioctahedral Al-rich 2:1 clay minerals [illite, dioctahedral smectite, muscovite, mixed-layered illite–smectite] are quantified together as the illite + smectite group (I + S) clay mineral [46].

The CEC was measured by the Co-hexamine technique following Bardon et al. [48]. The measured CEC value was used to quantify the smectite-equivalent component (%S) in the bulk rock I + S mineral group, following the method suggested by Środoń [49]. Total organic carbon (TOC) content and organic matter (OM) characterization (type and thermal maturity) were obtained commercially by Weatherford Laboratories, Houston, TX, using Leco TOC and the RockEval II methodology. OM content (wt.%) was calculated from TOC based on the assumption that typical carbon concentration in OM in sedimentary rocks is 83% [50].

3.2. Materials

Fifty six samples from two different gas shale plays were analyzed for total porosity using the WIP technique. The samples were taken from unpreserved core and do not represent the hydration state and saturation under reservoir conditions.

Sample Set 1 (SS1) consisted of 22 samples from two wells drilled in a Silurian gas shale play in Eastern Europe. The samples are composed mostly of I + S (32–49 wt.%), quartz + feldspar (30–52 wt.%), with up to 20 wt.% of carbonate minerals (calcite and dolomite). No sulfates or halides have been detected with XRD. The I + S clay species contains <5% expandable smectite layers. The TOC content ranges from 1.0 to 6.0 wt.%. The lack of any peak in the RockEval S2 pyrograms from the samples indicate that the OM in sample set is thermally very mature with no pyrolysable OM (Fig. 4a).

Sample Set 2 (SS2) consisted of 34 samples from a well drilled in the Jurassic Haynesville Shale gas play in East Texas, USA. The samples are composed mostly of I + S clay (21–60 wt.%), quartz + feldspar (13–34 wt.%), with variable amount of carbonate minerals (up to 59 wt.%; calcite, ankerite and excess-Ca dolomite with minor amounts of siderite). No sulfates or halides have been detected with XRD. The I + S clay species contains from <5% up to 9% expandable smectite layers. The TOC ranges from 0.5 to 6.3 wt.%. The RockEval II measurements indicate that the OM is thermally mature but, not as mature as SS1. The highly variable RockEval S2 pyrogram patterns for these

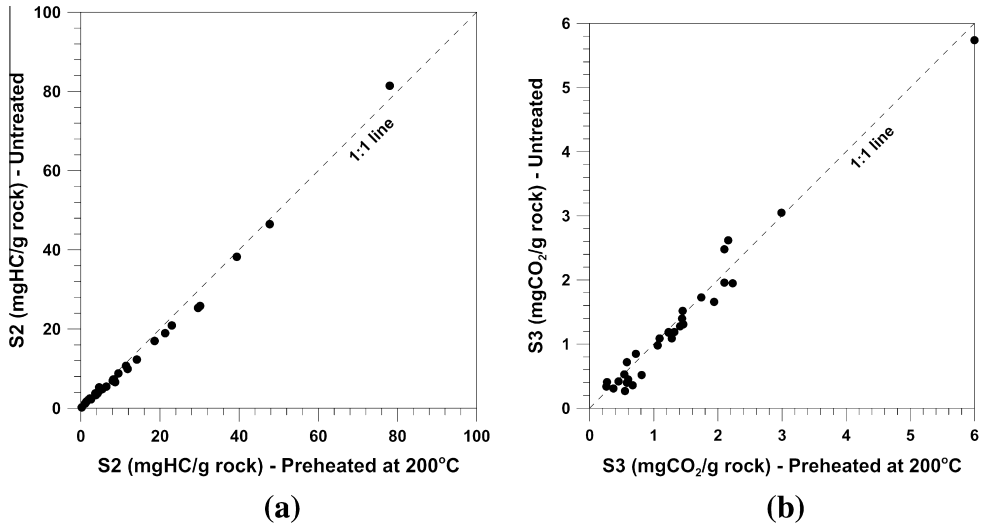

Fig. 3. Comparison of RockEval II (a) S2 and (b) S3 parameters measured before and after preheating at 200 °C on thirty organic rich shale samples from Baltic Basin.

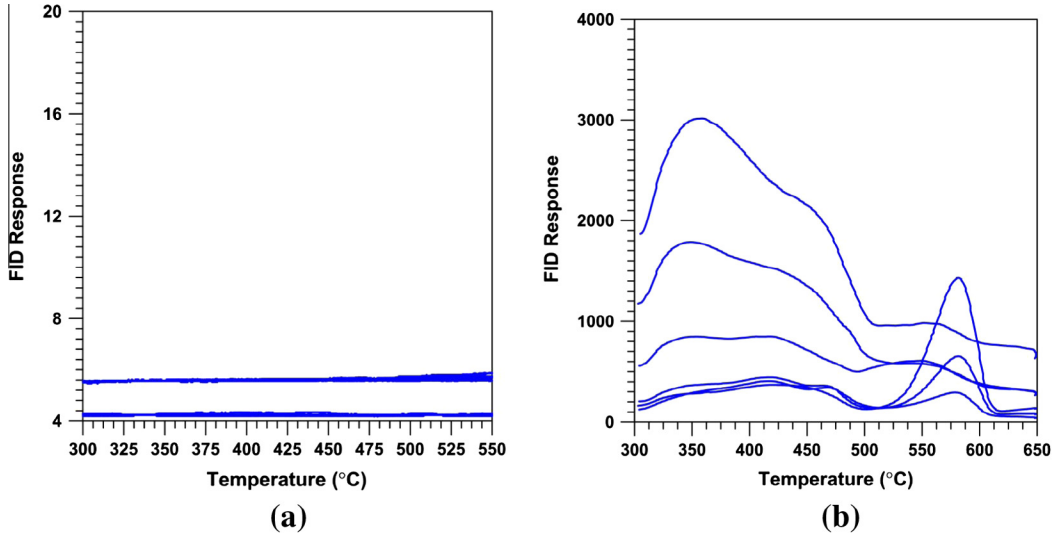

Fig. 4. RockEval II S2 pyrograms of different representative samples from the (a) Eastern European Silurian Shale (**SS1**) and (b) Haynesville Shale (**SS2**). The lack of any peak in S2 for SS1 samples suggest extremely mature OM with no pyrolysable kerogen. The presence of low temperature peak in SS2 indicates mature organic matter with high percentage of solid bitumen.

samples (Fig. 4b) suggest the OM is heterogeneous and has a significant amount of solid bitumen, indicated by dominant relatively low temperature S2 peaks between 350 and 450 °C [51].

3.3. WIP measurement and calculations

The experimental procedure (Fig. 5) and the parameters (*e.g.* sample size and mass, pretreatment time, saturating pressure and duration, etc.) reported here are the optimum values obtained from this study, and will be referred to as "adopted protocol". However, the parameters can be varied depending upon the requirements. The samples were preheated in a vacuum oven at 200 °C overnight (12–16 h) in order to remove all pore fluids. The dry weight of the sample ($DryWt_{Air}$) was measured after heating it at 200 °C for 15 min in a moisture analyzer (Mettler Toledo HB43^{TM}, readability 0.1 mg). Prior to saturation, the samples were degassed under vacuum of less than 1.33 Pa (10 μmHg) overnight inside the saturator and then they were saturated with DI water under 13.7 MPa (2000 psi) pressure for 24 h. The water saturated sample weight in air ($SatWt_{Air}$) and the submerged weight of saturated sample in DI water ($SatWt_{Sub}$) were measured in a conventional jolly balance set-up (Mettler Toledo XS^{TM}, readability 0.01 mg).

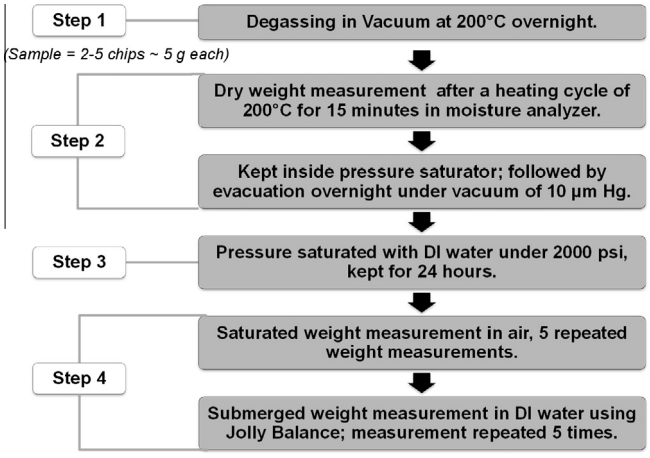

Fig. 5. Flow chart summarizing the analytical procedure steps followed in the WIP technique.

The water-saturated bulk density (ρ_B) of the sample is calculated using Eq. (2).

$$\rho_B = \left[\frac{SatWt_{Air}}{SatWt_{Air} - SatWt_{Sub}} \times \left(\rho_{H_2O} - \rho_{air}\right)\right] + \rho_{air} \quad (2)$$

where ρ_{H_2O} is the density of water at the measurement temperature T °C and ρ_{air} is the air density (0.0012 g/cm^3). ρ_{H_2O} is calculated using Eq. (3), obtained by fitting a second order polynomial to the published water density data [52].

$$\rho_{H_2O} = -0.0000053\ T^2 + 0.0000081\ T + 1.0001627 \quad (3)$$

where T is temperature of the water during measurement. The anhydrous grain density (ρ_G) is determined from the completely dehydrated sample weight in air and the completely saturated sample submerged in water:

$$\rho_G = \left[\frac{DryWt_{Air}}{DryWt_{Air} - SatWt_{Sub}} \times \left(\rho_{H_2O} - \rho_{air}\right)\right] + \rho_{air} \quad (4)$$

The porosity (ϕ_{WIP}) of any sample measured by WIP is determined by the relationship:

$$\phi_{WIP} = \frac{(\rho_B - \rho_G)}{(\rho_{H_2O} - \rho_G)} \times 100 \quad (5)$$

The porosity measured by WIP is the total water accessible porosity, including water adsorbed on clay surfaces, which includes the interlayer space in the expandable clay minerals and external surfaces of crystallites in non-expandable clay species (*i.e.* clay-bound water).

The weight measurements of the saturated samples in the jolly balance ($SatWt_{Air}$ and $SatWt_{Sub}$) were repeated at least five times for each study sample to evaluate the experimental uncertainties. The dry weight ($DryWt_{Air}$) was measured only once for each sample, however, based on repeated measurements of standard weights, a conservative uncertainty of 0.005 g was used for the dry weights. These uncertainties were carried through in the subsequent calculations using the law of propagating of uncertainty [53] to obtain the expanded uncertainty in the total porosity

measurements. The reported uncertainty defines the interval having a level of confidence of 95.45% ($\pm 2\sigma$ or standard deviation interval from the mean). Detailed descriptions of the WIP procedure are presented in Appendix B.

3.4. Reproducibility test

A test was performed on samples from SS1 with different chip sizes and saturating conditions to find the optimum parameters and to evaluate the reproducibility of the technique (see summary in Table 2). In Test 1 and Test 2, different sub-samples within a core-depth interval of 5 cm were used, however, the sample (chip) sizes were changed. Test 3 was repeated on exactly the same rock chips that were used in Test 2.

The last step of the WIP measurement is weighing the saturated rock chips submerged in water and in air. The saturated weight in air measurement requires removal of surface water. Prolonged exposure to room conditions and aggressive brushing could create the potential for operator bias in the measured weights. A test was designed to determine the sensitivity of the measurements to operator bias. Five samples were randomly selected and measured using WIP in a blind test by three separate operators.

3.5. Swelling test

Saturating these clay rich lithologies with DI water may potentially induce swelling and affect the bulk density measurements. A test was done to compare the bulk volumes of a different set of samples from the same formations before and after saturation with DI water. The bulk volume of the 42 irregular shaped chip samples from the Eastern European Silurian shales were measured using the Archimedes method. Seventeen cylindrical mini-plug core samples (diameter approximately 1 cm) were cut from the Haynesville conventional core. The bulk volume of these mini-plug samples were obtained both by caliper measurements and the Archimedes method. The samples were saturated using the same protocol as in the WIP technique.

3.6. Other porosity measurements

Depending on sample availability, WIP results were compared with other commonly used mudrock measurements, including the GRI and MIP techniques. The measurements were done on depth-equivalent samples, however the sample masses were different for the different procedures. Porosity by the GRI technique was done by a commercial vendor using ~300 g of sample representing core-depth interval of about ~15 cm, in contrast to the spot samples of about 10 g (within a maximum 5 cm interval) used for WIP and MIP.

MIP experiments were made using a Micromeritics AutoPore IV 9500™ porosimeter. A 3–5 g sample was kept in an oven at 110 °C overnight and then degassed at less than 6.6 Pa (50 μmHg) evacuation pressure for at least 30 min in the instrument. The samples were not crushed but small chips were used. Pore volumes are measured by intruded mercury volume at discrete pressure steps up to 413.7 MPa (60000 psi). Every pressure point was equilibrated below 0.001 μL/g/s intrusion rate. A conformance correction was done following the Bailey method as described in Comisky et al. [12].

4. Results

4.1. Reproducibility test

Despite significant differences in some of the experimental conditions, bulk density and grain density measurements performed on the SS1 samples using three different protocols are indistinguishable within the uncertainty interval (Fig. 6). Porosity calculations from these data using Eq. (5) are also highly consistent with a 0.41 p.u. average difference in the maximum and minimum measured porosity. The difference between the measured porosity can be accounted by the measurement uncertainties and the mean porosity values are reproducible within range of experimental uncertainty with a few exceptions. Sample 11 shows a maximum difference of 0.85 p.u., and Sample 16 shows a difference of 2.03 p.u. A repeated measure ANOVA test on the WIP data indicates that there is no significant difference between the different tests (see statistical test results in Appendix C, Table C.1).

Comparison between Test 2 and Test 3 (repeated measurements on same exact samples) shows consistently higher porosity values are obtained in the Test 3 samples, which were subjected to dehydration and saturation for the second time (Fig. 7a). This difference in porosity between Test 2 and Test 3 ranges from −0.07 to 0.83 p.u. with a mean of 0.47 p.u. The grain density values do not change (Fig. 7b), but there is systematic decrease in the bulk density values of the Test 3 samples compared to Test 2 (Fig. 7c). This is supported by the paired *t*-test results (see statistical test results in Appendix C, Table C.2) on these samples where bulk density values differ significantly, while the grain density variation is not significant. The differences observed in the WIP values may be due to micro fractures or swelling from repeated sample saturation and dehydration, because this would not affect the grain density, but would decrease the bulk density of the samples.

The results of the reproducibility test for the operator bias indicate there is no discernible trend in the data that can be attributed

Table 2
Test conditions for the reproducibility test.

Test #	Total sample mass (g)	Samples & chips description	Vacuum system used	Saturation system used	Operator	Additional comments
Adopted protocol	~10–11	Samples from a depth interval Individual Chip size: ~5.0 g	High vacuum	Pressure saturator, 2000 psi	3	$DryWt_{Air}$ measured after oven drying
Test 1	~4.5–5.5	Different sample from same sampling interval Individual Chip size: ~0.5 g	Low vacuum	No pressure, Bench top	1 and 2	$DryWt_{Air}$ measured by dring the saturated samples after jolly balance measurement
Test 2	~5–6	Different sample from same sampling interval Individual Chip size: ~2.5 g	Low vacuum	Pressure saturator, 2000 psi	3	$DryWt_{Air}$ measured by dring the saturated samples after jolly balance measurement
Test 3	~5–6	Exactly same samples re-measured after Test 2	High vacuum	Pressure saturator, 2000 psi	3	Samples kept in water saturated for 2 weeks before analysis

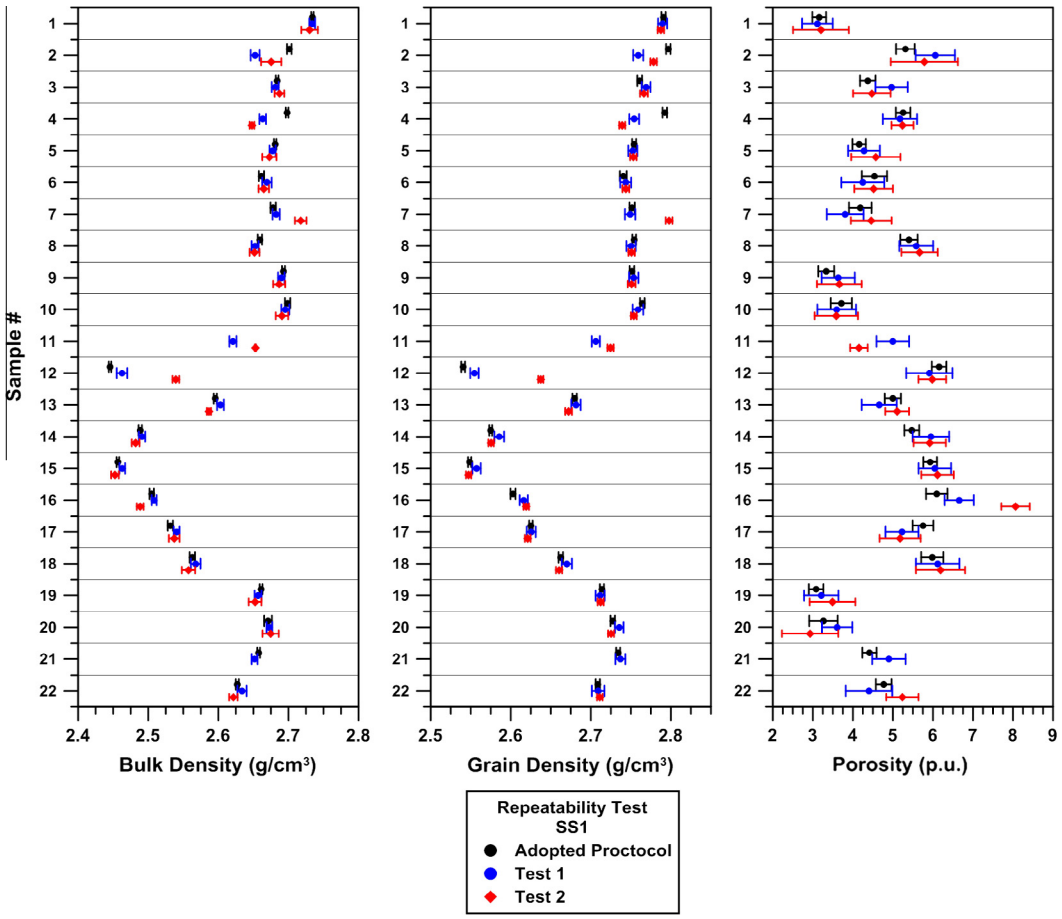

Fig. 6. Measured bulk density, grain density and porosity values for the 22 test samples from SS1 using the adopted WIP protocol, Test 1 and Test 2. The errors bars indicate expanded measurement uncertainty with 95.45% confidence interval range.

to a specific operator (Fig. 8). The average difference in WIP porosity measurements is 0.21 p.u. and the largest disparity is 0.5 p.u. for two samples (Sample 1 and Sample 4). However, in all the samples the propagated uncertainties are large enough to account for the difference in the measured WIP porosity values.

4.2. Swelling test

The bulk volume of fifty nine samples, measured by two independent methods (caliper measurements and Archimedes' volume), are consistent before and after saturation with DI water (Fig. 9a). The bulk volumes of both pre- and post-saturated Haynesville mini-plug samples measured by calipers are consistent with that obtained by Archimedes method, validating the accuracy of the measurements (Fig. 9b). The average volume change observed after saturation is 0.92% (±2.29%, sample size $n = 59$). The maximum increase in bulk volume due to saturation is 3.91%, which translates into a 0.04 p.u. bias in measured porosity. Therefore, the effect of potential swelling of rock during saturation with DI water falls well within the measurement uncertainty of the measured porosity values.

4.3. WIP data of the sample sets

The bulk density values from SS1 range from 2.446 to 2.734 g/cm^3. Note that the measured bulk density is with full DI water saturation and does not represent the formation in-situ bulk density. The grain density values of SS1 range from 2.540 to 2.797. The total porosity calculated from SS1 ranges from 3.08 to 6.16 p.u. In samples with low OM content, the total porosity increases with increasing clay content (Fig. 10a). The samples with the higher OM content have the higher total porosity (Fig. 10a and b). The total porosity is inversely correlated with total carbonate mineral content (Fig. 10c).

The bulk density values in SS2 range from 2.432 to 2.727 g/cm^3. The grain density values range from 2.527 to 2.845 g/cm^3. The total porosity values range from 3.45 to 12.68 p.u. There is an inverse correlation between the total porosity and carbonate mineral content (Fig. 11a and c). Total clay content shows in general a positive correlation with the WIP porosity, however, the high clay content samples with low carbonate content show a constant range of WIP values (Fig. 11a). OM content does not show any correlation with WIP porosity in the Haynesville samples (Fig. 11b).

4.4. Comparison of WIP with GRI and MIP measurements

To compare with other methodologies, porosity was obtained commercially by the GRI technique for nine SS1 samples, and 24 SS2 samples. The total porosity and grain density values obtained for SS1 by the WIP method are consistently higher than those for the comparable GRI samples except for one high OM content sample (Fig. 12a and b). Two distinct trends can be identified in the SS2 data. In general, samples with lower OM content have slightly higher WIP porosity values compared to GRI porosity, while samples with high OM have higher GRI porosity values (Fig. 13a). A similar trend is found in the grain density values (Fig. 13b). Samples with low OM content have nearly the same grain density values obtained by both methods, but the samples with highest OM have distinctly higher grain density values from the GRI technique.

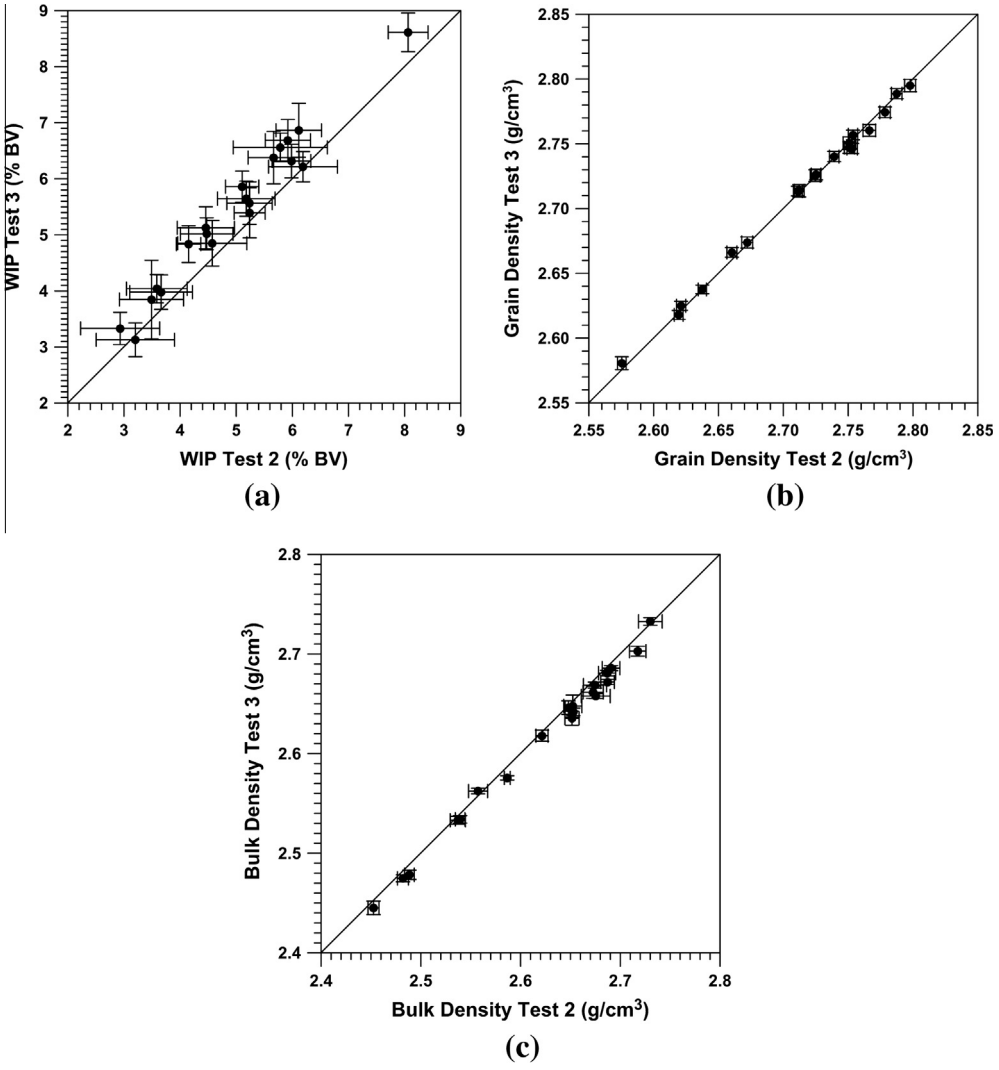

Fig. 7. Comparison of measured (a) porosity (b) grain density and (c) bulk density on exact same samples between Test 2 and Test 3. Repeated measurement on the same samples for the second time (Test 3) gives higher porosity values compared to that measured for the first time (Test 2). The 1:1 comparison line is marked in the plots.

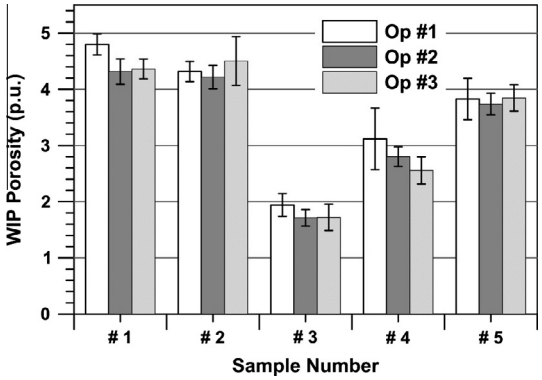

Fig. 8. Measured WIP data of five randomly selected samples by three different operators.

Porosity values using the MIP technique were obtained for the 22 samples in SS1, and from 13 samples from SS2. Comparison of measured porosity and grain density data shows that MIP porosity and grain density values are consistently lower relative to that measured by for all samples (Fig. 14a and b). The difference in porosity values ranges from a minimum of 2.7 p.u. to a maximum of 4.9 p.u. for SS1 and from 2.4 p.u. to 7.1 p.u. for SS2.

5. Discussion

5.1. Precision and accuracy of the WIP technique

Reproducibility tests demonstrate that the WIP technique is precise and reproducible. Optimization of the experimental methodology reduces the absolute experimental uncertainty (95.45% confidence interval or $\pm 2\sigma$ interval from the mean) to be ±0.2–0.3 p.u. with an average of ±0.22 p.u. (Fig. 6). The operator bias in the porosity measurement is within the experimental uncertainty (Fig. 8). The reported standard error for GRI porosity measurements range from 0.5 p.u. [5,6,8] to ~1.5 p.u. [7,9]. At least a part of the error is due to the lack of standardized operating procedures for GRI measurements among commercial laboratories.

The accuracy of the WIP technique depends on the complete saturation of the samples. The high penetration coefficient of DI water (Table 1) makes it the best choice of saturating fluid to achieve complete saturation, assuming that water is the wetting phase with a zero contact angle. There is concern that water may not completely penetrate the OM hosted pore system. Passey et al. [8] speculated that the organic pore may be hydrocarbon wet, while Schimmelmann et al. [54], Siskin et al. [55] and citations within, reported that at low temperatures hydrogen in water

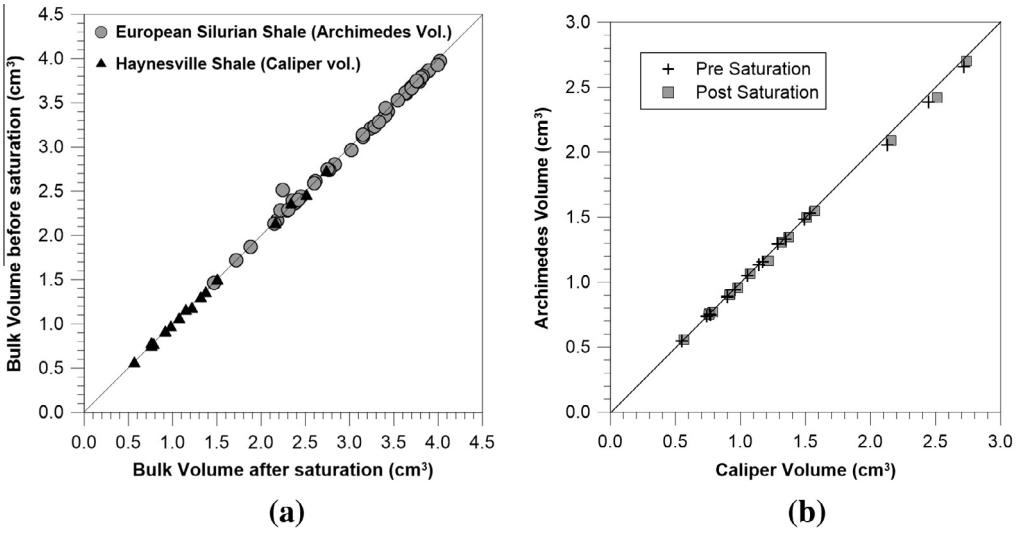

Fig. 9. (a) Comparison of bulk volume measured on the samples before and after saturation with DI water. The bulk volume of the European Silurian Shale were measured by Archimedes principle by immersing in DI water and the Haynesville mini-plug samples were measured by calipering the diameter and height. (b) Comparison of caliper measurements and Archimedes volume on pre-0 and post-saturated Haynesville mini-plug samples.

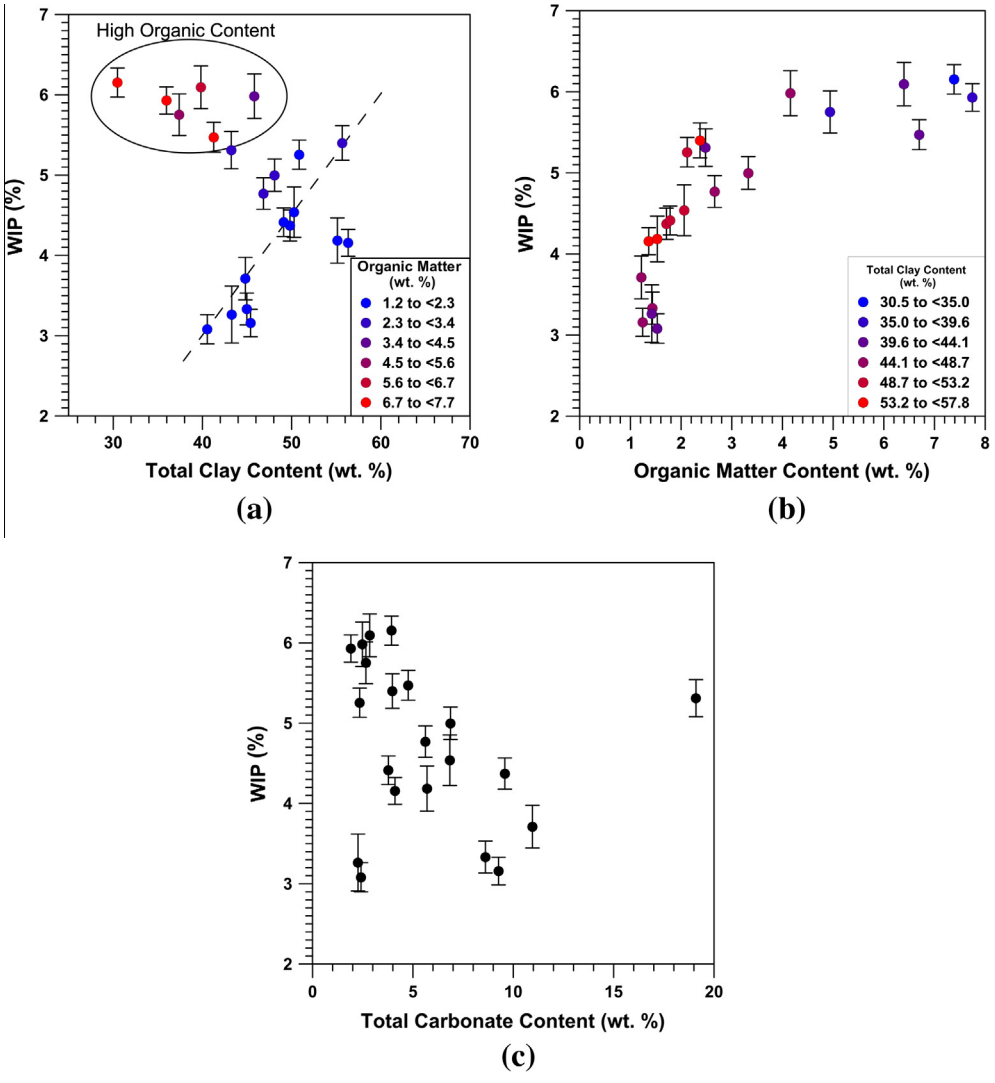

Fig. 10. Compositional controls on total porosity of shales from the Eastern European Silurian gas shale formation (SS1). (a) Total porosity as a function of total clay content (wt.%). The samples are color-coded by their OM content (wt.%). The dotted line indicate general trend and not a linear fit. (b) Total porosity as function of OM content (wt.%), samples color coded by their total clay content. (c) Total porosity as a function of total carbonate content (wt.%).

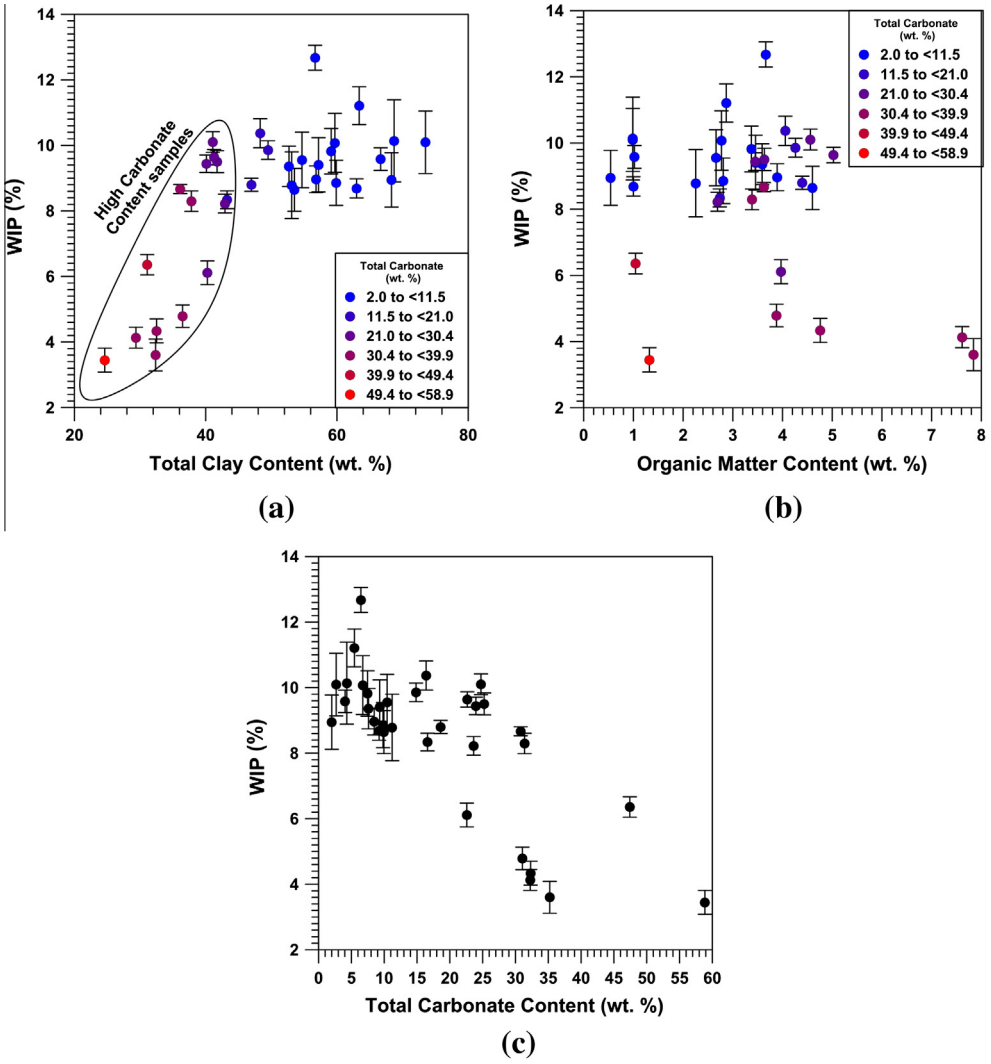

Fig. 11. Compositional controls on total porosity of shales from the Haynesville Formation (SS2). (a) Total porosity as a function of total clay content (wt.%). The samples are color-coded by their total carbonate content (wt.%). (b) Total porosity as function of OM content (wt.%), samples color coded by their total carbonate content. (c) Total porosity as a function of total carbonate content (wt.%).

molecules exchange with organic hydrogen, most of which is bound to NSO–functional groups in OM. In the WIP procedure, the samples are pretreated to remove liquid hydrocarbon prior to saturation with water. Water can enter into the OM pores without displacing a fluid that might have more affinity for the environment; this is not the issue of *displacement* but entering free space. Water adsorption studies on synthetic carbon based materials provides information that can be applied to water adsorption behavior of natural OM. Significant water adsorption by capillary condensation was reported for several types of activated nanoporous carbons [56–59] and carbon nanotubes [60]. The capillary condensation of water occurs from the hydrogen bonding of water molecules with polar oxygen-containing groups on the carbon materials to form clusters which grow in size until there is full condensation of water in the pore space [57,61–63]. Because of the abundant polar oxygenated functional groups in OM at all levels of maturity, along with its open and porous structure, there is no reason to expect that water would not fill its pore system. Recent molecular simulation studies of water in kerogen pores suggested pore filling by capillary condensation occurs in pores as small as 1.2 nm [64]. In the present study, no decrease in porosity was observed with increasing OM content in either sample set. Instead, the positive correlation between OM content and WIP porosity was observed for SS1 samples (Fig. 10a and b). These observations suggest that water can access the OM hosted porosity.

No significant amount of swelling was observed in the studied shale samples. Gas shale formations generally have high thermal maturity and advanced diagenesis with all detrital smectite transformed to illite with minimal expandable layers (e.g. [65]). This, along with a high level of compaction and cementation, minimizes the swelling of these formations.

5.2. Comparison between WIP and other porosity measurements

To assess the accuracy of the WIP method, the results were compared with those obtained by other measurement techniques (GRI and MIP). Comparison between WIP and MIP results indicate that MIP systematically underestimates the porosity and grain density of the samples studied. In most gas shales, the complete pore system cannot be accessed by mercury during the MIP measurements [13]. MIP measurements done on plugs and rock chips suggest incomplete mercury intrusion [12,13]. Application of MIP on crushed powder tends to give systematically higher porosity than that measured on plugs and chips [12].

Comparison of GRI and WIP porosity measured on samples for same core depth shows that WIP porosity has higher values than

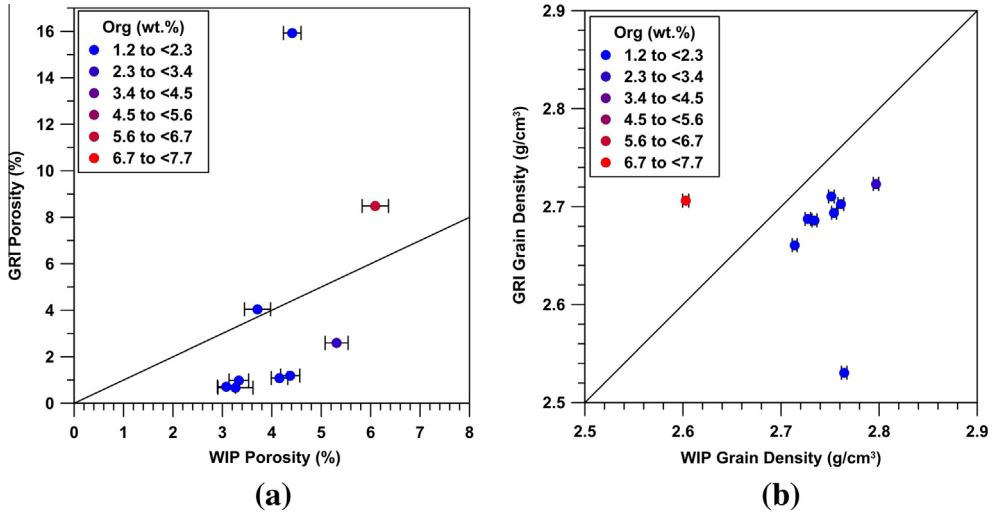

Fig. 12. Comparison of (a) measured total porosity and (b) measured grain density of the samples from SS1 by the WIP and GRI techniques. The 1:1 comparison line is marked by dotted line in the plots.

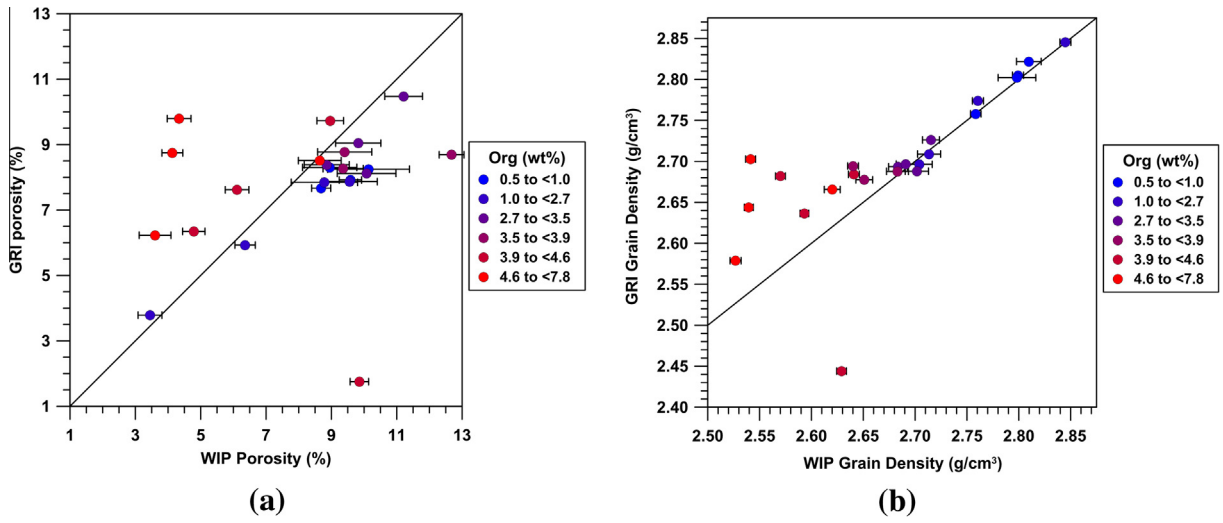

Fig. 13. Comparison of (a) measured total porosity and (b) measured grain density of the samples from SS2 by the WIP and GRI techniques. The 1:1 comparison line is marked by dotted line in the plots..

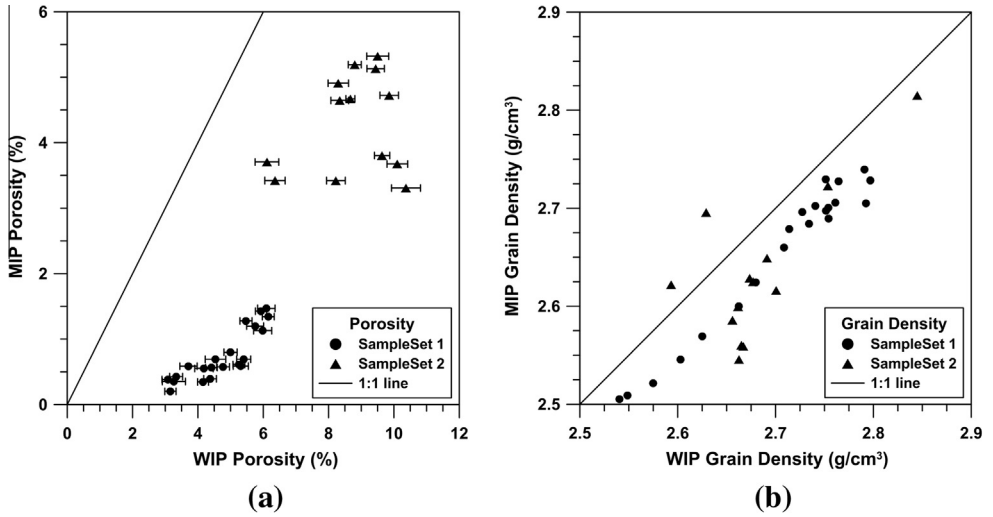

Fig. 14. Comparison of (a) measured total porosity and (b) measured grain density of the samples from SSS1 (circles) and SS2 (triangles) by the WIP and MIP techniques. The 1:1 comparison line is marked by dotted line in the plots.

GRI porosity for low organic content rocks (<3.0 wt.%), but an opposite trend exists in high organic content samples. The WIP grain density values for low OM content rocks from SS1 are higher than GRI grain density values by ~0.05 g/cm^3 (Fig. 12b). This difference is probably due to the uncertainty in GRI measurements from an unknown quantity of water molecules which may not be removed or were adsorbed before injection of the helium measurement gas. In SS2, there is a good match between WIP and GRI grain density values for low organic content samples. However, in the high OM samples there is systematically higher grain density values from the GRI technique. The probable reason is the solvent extraction treatment used in the GRI procedure removes a portion of solid OM that is a part of the rock matrix (Fig. 1). This increases porosity and skews the high OM content containing samples to higher grain density values. Based on the proportion of S2 recorded in the natural sample and the samples after Dean Stark procedure (Fig. 1), the solid OM fraction removed could account for ~0.5 p.u. excess porosity, assuming an OM density is estimated at 1.1 g/cm^3.

Another possible cause is the selective removal of the lighter, lower density, and fine grained material during the crushing of samples and subsequent sieving in the GRI procedure, which may create a bias toward the higher density components. The OM in the gas shale lithologies may tend to be ground into smaller grains during the crushing stage which are discarded during sieving.

5.3. Advantages of WIP technique

Significant advantages of the WIP method include: (i) all required measurements are conducted on the same portions of sample, (ii) no crushing is required and there is no preferential removal of material by sieving, and (iii) only 10–15 g of material is needed. Moreover, gravimetric measurements are more direct and precise compared to volumetric measurement techniques such as helium pycnometry. Gas based volumetric measurement are prone to leaks and temperature fluctuations in the system and generally requires frequent calibration of the reference volume. The water activity (or RH) environment during the saturation (100% water activity) and dehydration (0% water activity) weight measurements are well controlled in the WIP methodology. Repeated measurements are obtained to quantify and report the experimental uncertainty of every porosity measurement. The WIP experimental procedure is simple and quick to implement, which makes it applicable for routine core measurements. The measured grain density, bulk density and porosity are precise and reproducible with the experimental uncertainty. The average absolute experimental uncertainty is ±0.22 p.u.

5.4. Limitation of WIP technique

WIP technique will overestimate the grain density and porosity in samples which contains a significant amount of water soluble naturally occurring minerals such as halite, which could dissolve during saturation. However, most gas shales generally have low halite content, which can be quantified from the chlorine content available from chemical analysis. The samples used in this study have a maximum chlorine content of 0.17 wt.% (mean 0.08 wt.%), which is equal to 0.37 vol.% of halite assuming 2.80 g/cm^3 whole rock grain density. In the studied samples the maximum possible bias in the porosity measurement is about 0.37 p.u., however, the actual value will be much lower and within the limit of experimental uncertainty. This method is not recommended for smectite rich shales or those with high illite–smectite expandability.

Creation of microcracks during sample handling is a possibility which would result in higher than actual porosity, but this would not affect the grain density. The bias in the porosity is within limits of the experimental uncertainty (Test 2 and Test 3, Fig. 7). Significant quantities of gypsum and other hydrated sulfates would result in higher mass loss after dehydration at 200 °C due to crystalline water loss.

6. Conclusions

A modified methodology using a DI water saturation and immersion technique was adapted to measure total porosity in gas shales. The results suggest that:

1. Measured porosity, grain density, and bulk density obtained by the WIP technique are precise and reproducible.
2. The average absolute experimental uncertainty in the WIP porosity measurement using the adopted protocol is ±0.22 p.u. This is lower compared to the reported uncertainty level of ±0.5 p.u. in porosity measurement by the industry adopted GRI technique.
3. Potential limitations include possible incomplete saturation, water soluble mineral dissolution, crystalline water removal from hydrated sulfates, and sample swelling. The possible influence of these factors on the measured total porosity of the samples is not significant.
4. Comparison of results from WIP and MIP measurements indicates that MIP systematically underestimate the porosity and grain density, because the significant fine scale pore volume in these gas shales cannot be accessed by mercury.
5. The Dean Stark pretreatment in the GRI method can dissolve a fraction of the solid organic matter, create porosity artefacts and increase the grain density compared to WIP.

Acknowledgements

We would like to thank members of OCLASSH consortium at Colorado School of Mines and Chevron ETC for financially supporting this project. We thank Prince Ezebuiro, Kymberli Correll, Farrell Garner and Sheven Poole for their help in collecting the data for the analysis.

Appendix A. Flow chart of GRI technique

Fig. A.1.

Appendix B. Water immersion porosity measurement – Adopted protocol

The following steps were followed during the WIP procedure.

STEP 1 – Sample preparation. The samples were prepared by cutting two to three rectangular shaped chips from core material of ~3–5 g each and a total sample weight of ~10 g. The chips were cut using a diamond blade to smooth out irregularities which would hold surface water outside the pore system. The samples were then heated in a vacuum oven at 200 °C overnight (12–16 h) in order to remove all volatile components (water and hydrocarbons).

STEP 2 – Dry sample measurement. The dry weight ($DryWt_{Air}$) was measured in a moisture analyzer (Mettler Toledo HB43^{TM} readability 0.1 mg) by heating the sample at 200 °C for 15 min and the dry weight recorded at the end of the heating cycle. Use of a moisture analyzer and measuring the dry weight at the 200 °C condition prevents re-adsorption of moisture from the air during the dry weight measurement. The weight of the sample was monitored at every 5 min during the heating cycle.

STEP 3 – Saturating the samples. After the dry weight measurement, the samples were saturated under pressure in a Vinci Manual pressure saturator™. The pressure saturation chamber was connected to an ultra-high vacuum pump to evacuate the air in the sample prior to the introduction of water to ensure maximum possible saturation. The samples were kept in vacuum of less than 1.33 Pa (10 μmHg) overnight. Following evacuation, DI water was introduced into the sample chamber of the pressure saturator and a pressure of 13.7 MPa (2000 psi) was applied. The samples were kept under this pressure for 24 h.

STEP 4 – Water saturated sample measurement. The samples were taken out of the pressure saturator and transferred in a water filled beaker to avoid exposure to air. The chip portions were analyzed for bulk density using a conventional high–precision jolly balance set up with a Mettler Toledo XS™ instrument that has a readability of 0.01 mg. The saturated samples were weighed five times while submerged in a beaker of DI water ($SatWt_{Sub}$). The immersion DI water is mixed with a drop of surfactant, provided by the jolly balance instrument manufacturer, per 100 mL of water to relieve the surface tension of water effecting the submerged weight measurement. The temperature of the immersion water was recorded. The saturated samples were then weighed at least five times in air ($Sat.Wt._{Air}$). The surface of the chips was gently blotted with a small fine bristle paint brush on weigh paper to remove surface water so there was no sheen left and care was taken to minimize the exposure in air to minimize loss of water by evaporation. The samples were placed back in DI water filled beaker in between the weighing to minimize prolonged exposure in air.

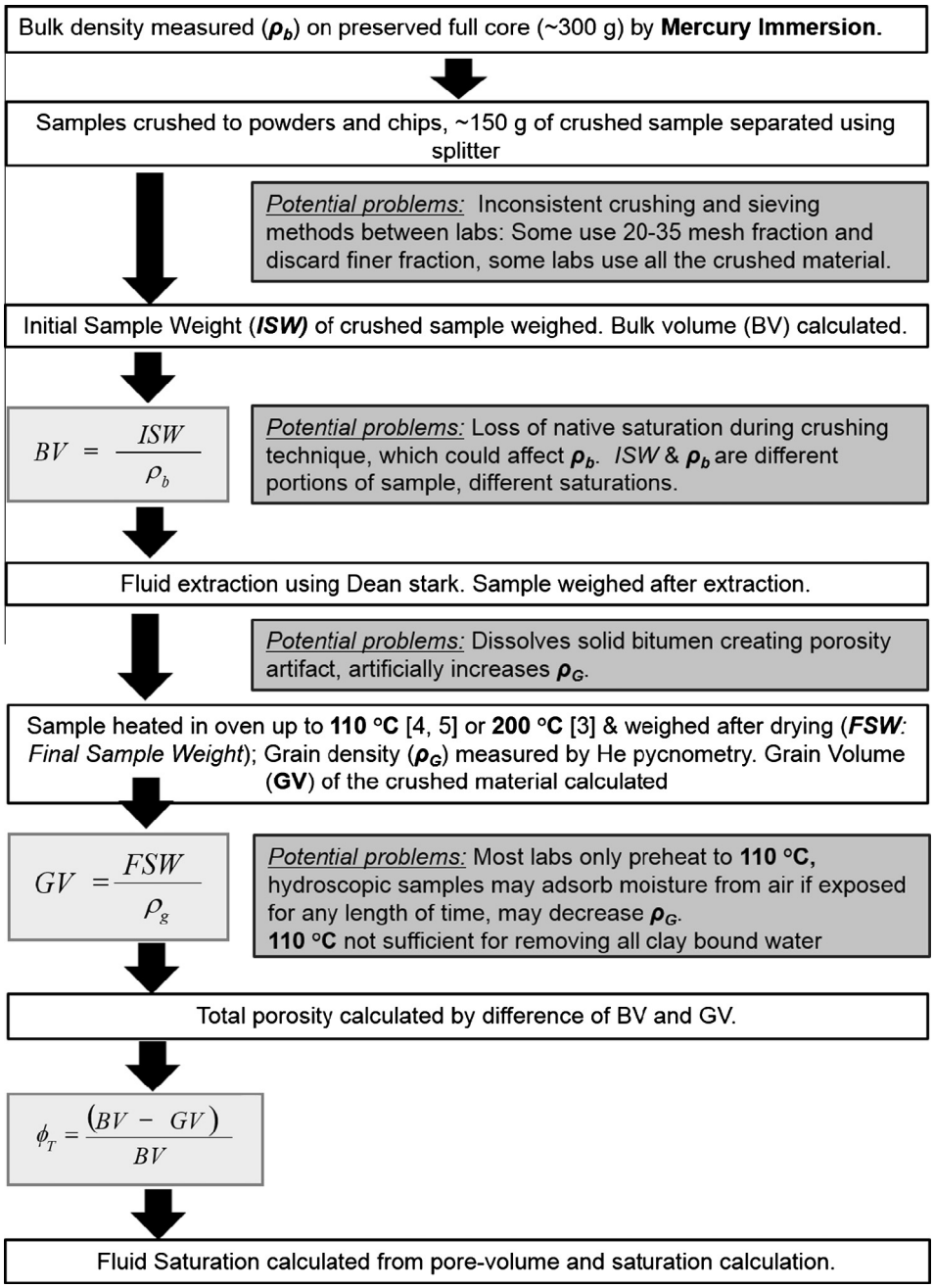

Fig. A.1. Flow chart summarizing the analytical procedure steps followed in the GRI technique (modified from [3–5]) . The potential pitfalls associated with each analytical step are also highlighted.

Table C.1
Results of repeated-measure ANOVA test comparing porosity values for the same samples under different test condition (AP: Adopted protocol, Test 1 and Test 2, Table 2). Samples SS1-11 and SS1-21 are excluded because of missing data, SS-16 omitted as outlier. Mauchly's Test of Sphericity indicated that the assumption of sphericity had not been violated, $\chi^2(2) = 1.133$, $p = 0.568$, and, therefore, repeated-measure ANOVA with sphericity assumption was used. There was no significant effect of different test condition (Table 2) on the measured porosity, $F(2,36) = 1.560$, p-value = 0.224. Type III SS = Type III sum of squares.; df = degrees of freedom; Noncent. Param. = Noncentrality parameter; Obs. Power = Observed Power.

Descriptive statistics	Mean	SD	N
WIP_AP	4.6737	1.0225	19
WIP_Test1	4.7163	1.0441	19
WIP_Test2	4.8058	1.0417	19

Mauchly's Test of Sphericity	Mauchly's W	Approx. Chi-Square	df	Sig.	Epsilon		
					Greenhouse - Geisser	Huynh - Feldt	Lower-bound
	0.936	1.133	2	0.568	0.939	1	0.5

Tests of within-subjects effects		Type III SS	df	Mean square	F-statistics	P- Value	Partial eta squared	Noncent. Param.	Obs. Power
Test conditions	Sphericity assumed	0.173	2	0.086	1.56	0.224	0.08	3.12	0.309
Error (Test)	Sphericity assumed	1.993	36	0.055					

Table C.2
Results of the paired-samples t-test conducted to compare the bulk density (BD), grain density (GD) and porosity (WIP) values of the samples under test condition Test 2 and Test 3 (Table 2). Samples SS1-6 and SS1-21 are excluded because of missing data. df = degrees of freedom, Sig. = significance.

Paired samples statistics		Mean	Sample size	Std. dev.	Std. error mean
Pair 1	BD_Test2	2.6203	20	0.0831	0.0186
	BD_Test3	2.6129	20	0.0825	0.0185
Pair 2	GD_Test2	2.7041	20	0.0723	0.0162
	GD_Test3	2.7046	20	0.0700	0.0157
Pair 3	WIP_Test2	4.9500	20	1.2577	0.2812
	WIP_Test3	5.4145	20	1.3532	0.3026

Paired Sample test	Paired Differences	Mean	Std. dev.	Std. error mean	95% C.I. of the diff.		t	df	p-Value
					Lower	Upper			
Pair 1	BD_Test2–BD_Test3	0.0075	0.0060	0.0013	0.0047	0.0103	5.557	19	0
Pair 2	GD_Test2–GD_Test3	−0.0005	0.0038	0.0008	−0.0022	0.0013	−0.596	19	0.558
Pair 3	WIP_Test2–WIP_Test3	−0.4645	0.2520	0.0564	−0.5825	−0.3465	−8.242	19	0

Appendix C. Statistical test results

Tables C.1 and C.2

References

[1] Schlumberger oilfield glossary; 2013 <http://www.glossary.oilfield.slb.com/en/Terms/p/porosity_unit.aspx>.
[2] Landis CR, Castaño JR. Maturation and bulk chemical properties of a suite of solid hydrocarbons. Org Geochem 1995;22(1):137–49.
[3] Luffel D, Guidry F. Core analysis results comprehensive study wells devonian shales: topical report. Tech. Rep., Restech Houston, Inc.; July 1989.
[4] Luffel DL, Guidry FK. New core analysis methods for measuring reservoir rock properties of Devonian shale. J Pet Technol 1992;44(11):1184–90.
[5] Luffel DL, Guidry FK, Curtis JB. Evaluation of Devonian shale with new core and log analysis methods. J Pet Technol 1992;44(11):1192–7.
[6] Karastathis A. Petrophysical measurements on Tight Gas Shales, PhD thesis; 2007.
[7] Sondergeld CH, Newsham KE, Comisky JT, Rice MC, Rai CS. Petrophysical considerations in evaluating and producing shale gas resources; In: SPE Unconventional Gas Conference, Pittsburgh, Pennsylvania, USA; 2010.
[8] Passey Q, Bohacs K, Esch W, Klimentidis R, Sinha S. From oil-prone source rock to gas-producing shale reservoir-geologic and petrophysical characterization of unconventional shale gas reservoirs. In: International oil and gas conference and exhibition in China; 2010.
[9] Spears RW, Dudus D, Foulds A, Passey Q, Sinha S, Esch WL. Shale gas core analysis: Strategies for normalizing between laboratories and a clear need for standard materials. In: Paper A, presented at the 52nd SPWLA annual logging symposium, Colorado Springs, CO; 2011.
[10] Bustin R, Bustin A, Cui A, Ross D, Murthy Pathi V. Impact of shale properties on pore structure and storage characteristics. In: SPE shale gas production conference; 2008.
[11] Sigal RF. A methodology for blank and conformance corrections for high pressure mercury porosimetry. Meas Sci Technol 2009;20(4):045108.
[12] Comisky J, Santiago M, McCollom B, Buddhala A, Newsham K. Sample size effects on the application of mercury injection capillary pressure for determining the storage capacity of tight gas and oil shales. In: Canadian unconventional resources conference; 2011.
[13] Sigal RF. Mercury capillary pressure measurements on Barnett core, submitted in petrophysics; 2013 <http://shale.ou.edu/Home/Publication> [accessed 29.03.13].
[14] API RP40. Recommended practices for core analysis; 1998.
[15] ASTM Standard C20-00. Standard test methods for apparent porosity, water absorption, apparent specific gravity, and bulk density of burned refractory brick and shape for boling water; 2010.
[16] ASTM Standard C830-00. Standard test methods for apparent porosity, liquid absorption, apparent specific gravity, and bulk density of refractory shapes by vacuum pressure; 2011.
[17] Franklin J, Vogler U, Szlavin J, Edmond J, Bieniawski Z. Suggested methods for determining water content, porosity, density, absorption and related properties and swelling and slake-durability index properties. Oxford: Pergamon Press; 1981. 79–94.
[18] Alexander J, Hall DH, Storey BC. Porosity measurements of crystalline rocks by laboratory and geophysical methods, Institute of Geological Sciences, Report EPNU; 1981. p. 81–10.
[19] Katsube TJ, Kamineni DC. Effect of alteration on pore structure of crystalline rocks; core samples from Atikokan, Ontario. Can Mineral 1983;21(4):637–46.
[20] Melnyk TW, Skeet AMM. An improved technique for the determination of rock porosity. Can J Earth Sci 1986;23(8):1068–74.
[21] Barnes KB. A method for determining the effective porosity of a reservoir-rock, vol. 10. School of Mineral Industries, State College, Pennsylvania; 1931 [chapter 1–12].
[22] Plummer FB, Tapp PF. Technique of testing large cores of oil sands. AAPG Bull 1943;27(1):64–84.
[23] Goldstrand P, Menefee L, Dreier R. Porosity development in the Copper Ridge Dolomite and Maynardville Limestone, Bear Creek Valley and Chestnut Ridge, Tennessee. Tech. Rep., Oak Ridge Y-12 Plant, TN (United States); Nevada Univ., Reno, NV (United States). Dept. of Geology; Appalachian State Univ., Boone, NC (United States). Dept. of Geology; Oak Ridge National Lab., TN (United States); 1995.
[24] Shapiro L. Rapid analysis of silicate, carbonate and phosphate rocks – revised edition, vol. 1401 of USGS Bulletin, US Government Printing Office; 1975.
[25] Brownell W. Procedures for the characterization of Devonian shales. In: Proc. first eastern gas shales symp US Dept. Energy, N.T.I.S., MERC/SP-77-5, US Dept. of Energy, Technical Information Center; 1977. p. 659–66.

[26] Nuhfer EB. Determination of density and porosity, United States Department of Energy, Morgantown, West Virginia, USA; 1979. p. 11–24 [chapter 4].
[27] Howard JJ. Porosimetry measurement of shale fabric and its relationship to illite/smectite diagenesis. Clays Clay Miner 1991;39(4):355–61.
[28] Katsube TJ, Scromeda N. Effective porosity measuring procedure for low porosity rocks. Geological Survey of Canada, Paper 91-1E; 1991. p. 291–7.
[29] T.J. Katsube, N. Scromeda, M. Williamson, Effective porosity of tight shales from the Venture Gas Field, Offshore Nova Scotia. Geological Survey of Canada, Paper 92-1D; 1992. p. 111–9.
[30] Dorsch J, Katsube TJ, Sanford WE, Dugan BE, Tourkow LM. Effective porosity and pore-throat sizes of Conasauga Group mudrock: application, test and evaluation of petrophysical techniques, No. ORNL/GWPO-021, Tech Rep, Oak Ridge National Lab., Environmental Sciences Div., TN (United States); 1996.
[31] Dorsch J, Katsube TJ. Effective porosity and pore-throat sizes of mudrock saprolite from the Nolichucky shale within Bear Creek Valley on the Oak Ridge Reservation: implications for contaminant transport and retardation through matrix diffusion, No. ORNL/GWPO-025, Tech Rep, Oak Ridge National Lab., Environmental Sciences Div., TN (United States); 1996.
[32] Gaucher E, Robelin C, Matray JM, Négrel G, Gros Y, Heitz JF, et al. ANDRA underground research laboratory: interpretation of the mineralogical and geochemical data acquired in the Callovian Oxfordian formation by investigative drilling. Phys Chem Earth 2004;Parts A/B/C 29(1):55–77.
[33] Washburn EW, Fooyitt FF. Porosity: III. Water as an absorption liquid. J Am Ceram Soc 1921;4(12):961–82.
[34] Washburn EW. The dynamics of capillary flow. Phys Rev 1921;17(3):273.
[35] Washburn EW, Bunting EN. Porosity: V. Recommended procedures for determining porosity by methods of absorption. J Am Ceram Soc 1922;5(1):48–56.
[36] Sato T, Watanabe T, Otsuka R. Effects of layer charge, charge location, and energy change on expansion properties of dioctahedral smectites. Clays Clay Miner 1992;40(1):103–13.
[37] Cooles GP, Mackenzie AS, Quigley TM. Calculation of petroleum masses generated and expelled from source rocks. Org Geochem 1986;10(1–3):235–45.
[38] Wilhelms A, Larter SR, Leythaeuser D. Influence of bitumen-2 on Rock-Eval pyrolysis. Org Geochem 1991;17(3):351–4.
[39] Noble RA, Kaldi JG, Atkinson CD. Oil saturation in shales: applications in seal evaluation, vol. 74101. Tulsa, Oklahoma, USA: The American Association of Petroleum Geologists; 1997. p. 13–30 [chapter 2].
[40] Deygout F. Volatile emissions from hot bitumen storage tanks. Environ Prog Sustain Energy 2011;30(1):102–12.
[41] Larter S. Some pragmatic perspectives in source rock geochemistry. Mar Pet Geol 1988;5(3):194–204.
[42] Drits VA, McCarty DK. The nature of structure-bonded H_2O in illite and leucophyllite from dehydration and dehydroxylation experiments. Clays Clay Miner 2007;55(1):45–58.
[43] Środoń J, McCarty DK. Surface area and layer charge of smectite from CEC and EGME/H_2O-retention measurements. Clays Clay Miner 2008;56(2):155–74.
[44] Derkowski A, Drits VA, McCarty DK. Rehydration of dehydrated–dehydroxylated smectite in a low water vapor environment. Am Mineral 2012;97(1):110–27.
[45] McCarty DK. Quantitative mineral analysis of clay bearing mixtures: the Reynolds Cup contest. IUCr CPD Newsl 2002;27:12–6.
[46] Środoń J, Drits VA, McCarty DK, Hsieh JC, Eberl DD. Quantitative X-ray diffraction analysis of clay-bearing rocks from random preparations. Clays Clay Miner 2001;49(6):514–28.
[47] Omotoso O, McCarty DK, Hillier S, Kleeberg R. Some successful approaches to quantitative mineral analysis as revealed by the 3rd Reynolds Cup contest. Clays Clay Miner 2006;54(6):748–60.
[48] Bardon C, Bieber M, Cuiec L, Jacquin C, Courbot A, Deneuville G, et al. Recommandations pour la détermination expérimentale de la capacité d'échange de cations des milieux argileux. Revue de Í Institut Francais Du Pétrole 1983;38(5):621–6.
[49] Środoń J. Quantification of illite and smectite and their layer charges in sandstones and shales from shallow burial depth. Clay Miner 2009;44(4):421–34.
[50] Jarvie DM. Total organic carbon (TOC) analysis. In: Merrill RK, editor. Treatise of petroleum geology: Handbook of petroleum geology, source and migration processes and evaluation techniques: AAPG, 1991, 113–118.
[51] Clementz DM. Effect of oil and bitumen saturation on source-rock pyrolysis: geologic notes. AAPG Bull 1979;63(12):2227–32.
[52] Haynes WM, Lide DR, Bruno T. CRC handbook of chemistry and physics 2012–2013. illustrated ed., vol. 93. CRC Press; 2012. p. 7–9 [chapter 6].
[53] Taylor BN, Kuyatt CE. Guidelines for evaluating and expressing the uncertainty of NIST measurement results. Natl Inst Stand Technol Tech Note 1297, 1994.
[54] Schimmelmann A, Lewan MD, Wintsch RP. D/H isotope ratios of kerogen, bitumen, oil, and water in hydrous pyrolysis of source rocks containing kerogen types I, II, IIS, and III. Geochim Cosmochim Acta 1999;63(22):3751–66.
[55] Siskin M, Katritzky AR, et al. Reactivity of organic compounds in hot water: geochemical and technological implications. Science (Washington) 1991;254(5029):231–7.
[56] Dubinin M. Water vapor adsorption and the microporous structures of carbonaceous adsorbents. Carbon 1980;18(5):355–64.
[57] Kaneko K, Hanzawa Y, Iiyama T, Kanda T, Suzuki T. Cluster-mediated water adsorption on carbon nanopores. Adsorption 1999;5(1):7–13.
[58] Alcañiz-Monge J, Linares-Solano A, Rand B. Mechanism of adsorption of water in carbon micropores as revealed by a study of activated carbon fibers. J Phys Chem B 2002;106(12):3209–16.
[59] Kimura T, Kanoh H, Kanda T, Ohkubo T, Hattori Y, Higaonna Y, et al. Cluster-associated filling of water in hydrophobic carbon micropores. J Phys Chem B 2004;108(37):14043–8.
[60] Naguib N, Ye H, Gogotsi Y, Yazicioglu AG, Megaridis CM, Yoshimura M. Observation of water confined in nanometer channels of closed carbon nanotubes. Nano Lett 2004;4(11):2237–43.
[61] Dubinin M, Serpinsky V. Isotherm equation for water vapor adsorption by microporous carbonaceous adsorbents. Carbon 1981;19(5):402–3.
[62] Ohba T, Kanoh H, Kaneko K. Water cluster growth in hydrophobic solid nanospaces. Chem – A Eur J 2005;11(17):4890–4.
[63] Cailliez F, Trzpit M, Soulard M, Demachy I, Boutin A, Patarin J, et al. Thermodynamics of water intrusion in nanoporous hydrophobic solids. Phys Chem Chem Phys 2008;10(32):4817–26.
[64] Hu Y, Devegowda D, Striolo A, Ho TA, Phan A, Civan F, Sigal R. A pore scale study decribing the dynamics of slickwater distribution in shale gas formations following hydralic fracturing. In: Unconventional resources conference – USA. The Woodlands, Texas, USA, sPE 164552-MS; 10–12 April 2013.
[65] Środoń J, Clauer N, Huff W, Dudek T, Banaś M. K–Ar dating of the lower palaeozoic K-bentonites from the Baltic Basin and the Baltic Shield: implications for the role of temperature and time in the illitization of smectite. Clay Miner 2009;44(3):361–87.